Thermohaline Stability and Fine Structure of the Gerlache Strait Waters, Antarctic Peninsula.

UNIVERSIDAD NACIONAL DE COLOMBIA

Julián Alberto Delgadillo Marín[1], Nancy Liliana Villegas Bolaños[2], Daniela Montaño Bello[3]

[1] Antarctic Affairs Study Group. National University of Colombia, Department of Geosciences, Bogotá, Colombia, e-mail: jadelgadillom@unal.edu.co
[2] National University of Colombia, Department of Geosciences, Bogotá, Colombia, e-mail: nlvillegasb@unal.edu.co
[3] Research group in Oceanology CENIT. National University of Colombia, Department of Geosciences, Bogotá, Colombia, e-mail: dmontanob@unal.edu.co

GEAA Grupo de Estudio en Asuntos Antárticos UN

GRUPO DE INVESTIGACIÓN EN OCEANOLOGÍA

ABSTRACT

The present study contributes to the knowledge of the water layers, the components of thermohaline stability and the vertical fine structure of the Gerlache strait waters. The region is located to the west of the Antarctic peninsula, between the Danco coast and the Palmer archipelago, between 64 - 65 °S and 61 - 64 °W. Data at a resolution of 0.25x0.25 was extracted from the World Ocean Atlas (WOA18) to analyze monthly and annually the Temperature (*T*, °C) and Salinity (*S*) of the climatological base period 1981 - 2010 for the study area. The depth and thickness of the quasi-homogeneous, thermocline, halocline, pycnocline, and lower layers were determined by calculating vertical gradients of *T*, *S*, and density (ϱ, kg/m³) in the northern, central, and southern sectors of the strait. Thermohaline stability (*E*) was evaluated using the Hesselberg-Svedrup criterion, identifying the contribution of the thermal (*Et*) and haline (*Es*) components to overall stability (*E*) and the Vaisala-Brunt Frequency (*N*). The vertical fine structure mechanisms were identified through the Stability Relation (*Rϱ*). The greatest oscillation of the thickness of the layers occurred in the central zone, where the maximum thermocline was 90 m in the austral summer and a minimum in winter. The halocline had a maximum thickness in autumn (220 m) and a minimum in spring (105 m). The pycnocline showed a thickness of around 300 m during the 12 months. The *Es* component represented the greatest contribution to *E*, exhibiting positive stability from 0 to 300 m and indifferent behavior to greater depths. The *N* values showed that the mixing processes take place mainly at the superficial level in summer and to a lesser extent in winter. The fine structure showed an Absolute Stability (*AS*) above 60 m, below 60 m Convection by Layers (*CL*) prevailed, and a Salt Fingers (*SF*) were observed from 300 to 325 m and 375 to 400 m in some stations. Future research suggestions are to analyze the vertical structure of the water column with in situ and reanalisis data to detail the dynamics of the currents and the distribution of the water masses in the Gerlache Strait.

Keywords: Thermocline, Hesselberg-Svedrup, Salt Fingers, Vaisala-Brunt Frequency, WOA18.

AREA OF STUDY, DATA AND METHODOLOGY

The Gerlache Strait is located to the West of the Antarctic Peninsula (WAP) between 64 - 65 °S and 61 - 64 °W (Fig. 1), it is about 6-32 km wide and 161 km long. Extending in-between the Danco coast and the Palmer archipelago. According to Garcia et al. (2002), the Palmer Trench with a depth of 500-1000 m demarcates its eastern limit connecting with the Bismarck Strait. In its central part depths are less than 500 m. To the east it borders the Bransfield Strait which has depths greater than 1000 m. A persistent superficial oceanic current its present across the strait at 10-18 cm/s and varies seasonally in a northeasterly direction towards the Bransfield Current (Zhou et al., 2002). The highest values of biomass and productivity are recorded both in the bays and in the center of the strait during the austral summer (Burkholder & Sieburth, 1961).

Data used are Temperature (*T*, °C) and Salinity (*S*) from the World Ocean Atlas (WOA18) with ¼° resolution for the 1981-2010 period (Locarnini et al., 2019; Zweng et al., 2018). Twelve stations (G1 - G12: Fig. 1, Table 1) were designated with available data to study the water column for *T* and *S* variables. This data allowed for the surface analysis of *T* and *S* in the strait, 5 stations covering the southwest (G1), central west (G2), central east (G4) and northeast (G8 and G12) zones were chosen to carry out transects and vertical profiles water column.

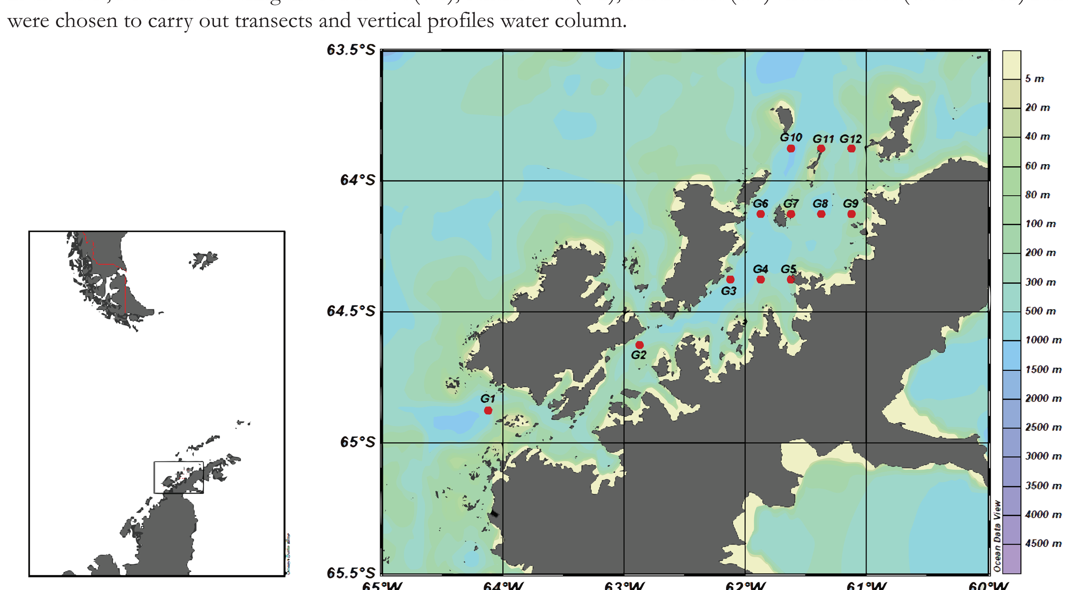

Fig. 1. Location of the Gerlache Strait. Reference points in red (stations G1 - G12) where *T* and *S* data for the water column from WOA18 (1981-2010) was extracted.

Table 1. Coordinates of the reference points (stations G1-G12) where *T* and *S* (1981-2010) from WOA18 were obtained.

Estación	Latitud	Longitud	Estación	Latitud	Longitud	Estación	Latitud	Longitud
G1	-64.875	-64.125	**G5**	-64.375	-61.625	**G9**	-64.125	-61.125
G2	-64.625	-62.875	**G6**	-64.125	-61.875	**G10**	-63.875	-61.625
G3	-64.375	-62.125	**G7**	-64.125	-61.625	**G11**	-63.875	-61.375
G4	-64.375	-61.875	**G8**	-64.125	-61.375	**G12**	-63.875	-61.125

The Hesselberg-Svedrup (*E*) criterion is calculated as shown in the following equation (Malinin (1998) in Villegas 2004).

$$E = \frac{\partial \rho}{\partial S}\frac{dS}{dz} + \frac{\partial \rho}{\partial T}\frac{dT}{dz} + \frac{\partial \rho}{\partial T}\frac{dT_a}{dz} \qquad (1)$$

Where, $\frac{\partial \rho}{\partial S}$ is the correction of the change in density for the change in salinity; $\frac{dS}{dz}$ is the vertical salinity gradient; $\frac{\partial \rho}{\partial T}$ is the correction of the density change for the temperature change; $\frac{dT}{dz}$ is the vertical temperature gradient; $\frac{dT_a}{dz}$ is the adiabatic temperature gradient.

The first part of equation (1) represents the contribution of *S* to the stability of the water column and is called *Es*, the two remaining members of (1) represent the contribution to the stability of *T* and are called *Et*, therefore:

$$E = E_s + E_t \qquad (2)$$

The sum of the Es and Et components is called the total thermohaline stability E and is a significant criterion to understand how the vertical stability in the ocean layers is affected between the warm and cold seasons of the year. If $E>0$ a stable equilibrium prevails, if $E<0$ it is unstable and if $E=0$ it is indifferent.

The criterion that characterizes the frequency of vertical oscillations in the stratified ocean is called the Vaisala-Brunt Frequency (*N*). Overall, the minimum values of *N* in the world ocean are between 10^{-3} and 10^{-4} 1/sec and the maximum values up to 10^{-2} 1/sec, for the seasonal thermocline. *N* is calculated by the equation:

$$N = \sqrt{\frac{g}{\rho}\frac{d\rho}{dz}} \qquad (3)$$

Where, $g \approx 9.81$ m/s² ; ϱ is density; dϱ/dz is the vertical density gradient.

The Density Ratio *Rϱ* criterion is calculated by the equation:

$$R_\rho = -\frac{E_s}{E_t} \qquad (4)$$

Four types of stratification are possible:

1. Total or absolute stability (*AS*): $\frac{dT}{dz} > 0, \frac{dS}{dz} < 0,\ Et > 0, Es > 0, R_\rho < 0$
2. Salt fingers stability (*SF*): $\frac{dT}{dz} < 0, \frac{dS}{dz} < 0,\ Et > 0, Es < 0, R_\rho > 0$
3. Convective stratification by layer (*CL*): $\frac{dT}{dz} > 0, \frac{dS}{dz} > 0,\ Et < 0, Es > 0, R_\rho > 0$
4. Total instability (*TI*): $\frac{dT}{dz} > 0, \frac{dS}{dz} < 0,\ Et < 0, Es < 0, R_\rho < 0$

The Density relation of the medium (*Rϱ*) for the water column is calculated according to the corresponding contributions of *Et* and *Es* in the stability *E*. Based on these values and the vertical gradients of *T*, *S* and ϱ, the fine structure of the water column in each of the stations is determined.

RESULTS

Annual climatological behavior of Sea Surface Temperature (SST, °C) and Sea Surface Salinity (SSS) for the period 1981-2010

Table 2 shows the maximum, minimum, amplitude and average values of the annual climatological behavior of the *SST* and the *SSS* for the period 1981-2010. Overall, higher values are identified in the southwestern zone with 1.75 °C (G1) and central with 2.00 °C (G2) and 1.75 °C (G4), lowest *SST* are observed in the northeast zone with 1.54 °C (G8) and 1.50 °C (G12). Mean *SST* values are recorded for the northeast zone (G6 and G7) with 1.67 °C and 1.62 °C respectively. Highest *SST* amplitudes occur in the southwestern areas with 3.36 °C (G1) and central areas with 3.58 °C (G2) and 3.47 °C (G4), lowest annual amplitudes are recorded in the northeast zone with 3.28 °C (G8) and 3.05 °C (G12).

Regarding the maximum and minimum of the *SSM*, Table 2 presents the highest values in the northeast zone with 34.37 (G12) and 34.38 (G8), lowest values are observed in the southwest zone with 34.16 (G1) and the central west zone with 34.24 (G2). Mean values were observed in the northeast and central east zones (G6 and G4) with 34.31 and 34.36 respectively. Highest annual *SSM* amplitudes are recorded in the southwestern zones with 0.97 (G1), and central with 0.74 (G2) and 0.75 (G4), smallest amplitudes are found in the northeast area with 0.65 (G8) and 0.58 (G12).

Table 2. Maximum, minimum, amplitude and average values of the annual climatological behavior of *SST* (°C) and *SSS* for the period 1981-2010 in Gerlache Strait stations, obtained with data from WOA18.

Gerlache Station	SST, °C				SSS, psu			
	Max	Min	Amplitude	Average	Max	Min	Amplitude	Average
G1	1.75	-1.61	3.36	-0.25	34.16	33.19	0.97	33.76
G2	2.00	-1.58	3.58	-0.12	34.24	33.50	0.74	33.83
G3	1.80	-1.73	3.53	-0.23	34.30	33.55	0.75	33.88
G4	1.75	-1.72	3.47	-0.16	34.36	33.61	0.75	33.93
G5	1.69	-1.73	3.42	-0.16	34.40	33.65	0.75	33.95
G6	1.67	-1.64	3.31	-0.20	34.31	33.68	0.63	33.97
G7	1.62	-1.61	3.23	-0.19	34.36	33.70	0.66	33.98
G8	1.54	-1.74	3.28	-0.26	34.38	33.73	0.65	33.99
G9	1.47	-1.59	3.06	-0.29	34.39	33.69	0.7	33.99
G10	1.60	-1.68	3.28	-0.17	34.32	33.81	0.51	34.01
G11	1.55	-1.59	3.14	-0.18	34.34	33.76	0.58	34.03
G12	1.50	-1.55	3.05	-0.17	34.37	33.79	0.58	34.07

Quasi-Homogeneous Layer (QHL): IsoThermal Layer (ITL) and IsoHaline Layer (IHL)

Fig. 2 shows the profiles of the multi-annual monthly average for the period 1981-2010 of *T* (°C) and *S* for the southwest (G1: Fig. 2a and Fig. 2b), central west (G2: Fig. 2c and Fig. 2d), central east (G4: Fig. 2e and Fig. 2f), northeast (G8: Fig. 2g and Fig. 2h) and northeast (G12: Fig. 2i and Fig. 2j) of the Gerlache Strait. In the first 150 m, the variation of the *T* and *S* of the most superficial waters in the Quasi-Homogeneous Layer (QHL) is observed, this due to the dominant mechanisms of atmospheric dynamics, the formation and melting of sea ice, among others. (Garcia et al., 2002). Below 150 m, the atmospheric effects are reduced and the *T* and *S* register more homogeneous and less dispersed values. The thermocline has its maximum thickness during the southern summer, and during winter (July and August) almost disappear as a result of thermal instability present in the water column. The halocline has its minimum thickness in spring (September), and its maximum in autumn (April).

The ISL presents its greatest thickness during the austral autumn (Table 3), extending from 0 to 12 -15 m in the areas of the strait (Figs. 2a-2j). The average value of this layer varies, being the highest of 0.46 °C in the southwest (G1), and the lowest of -0.10 °C in the northeast (G8). In the other seasons of the year, the ISL extends from 0 to 5 - 7 m (Figs. 2a-2j). The average *T* of the highest ISL is recorded in summer with 1.28 °C in the central west zone (G2) and the lowest in spring at -1.46 °C in the southwest (G1).

Table 3. Seasonal values of the thickness (m) and the average temperature (*T*, °C) of the Isothermal Layer (ITL) and the thermocline in the Gerlache Strait. Data from WOA18 for the period 1981-2010.

Gerlache stations	Layer	Summer (DJF)		Autumn (MAM)		Winter (JJA)		Spring (SON)	
		Thickness, m	Average T, °C	Thickness, m	Average T, °C	Thickness, m	Average T, °C	Thickness, m	Average T, °C
G1	ISL	7	0.99	15	0.46	5	-1.09	7	-1.46
	Thermocline	63	0.44	45	0.34	10	-0.20	17	-1.60
G2	ISL	5	1.28	12	0.27	5	-1.07	5	-1.22
	Thermocline	78	0.58	58	0.10	12	-0.70	20	-1.48
G4	ISL	5	1.17	12	-0.02	5	-1.24	7	-0.97
	Thermocline	103	0.48	71	0.12	8	-0.82	13	-1.33
G8	ISL	5	1.05	12	-0.10	5	-1.25	5	-1.05
	Thermocline	120	0.35	72	0.04	13	-0.82	15	-1.31
G12	ISL	5	1.06	12	0.00	5	-1.17	5	-0.93
	Thermocline	220	0.33	180	-0.01	10	-0.78	18	-1.17

The IHL registers its greatest thickness in spring (Table 4), especially in the northeast area (Figs. 2h and 2j) with 67 m and 34.25 average *S* (G8), on the other hand the southwest (G1) registers 28 m and 34.05 (Fig. 2b). The lowest IHL thickness values are observed in the austral summer, extending from 0 to 8 m with a greater thickness in the northeast zone (G12) and a higher *S* with values of 34.00 (Figs. 2h and 2j) in contrast to the southwest (Fig. 2b), where the average salinity is 33.42 (G1).

Table 4. Seasonal values of the thickness (m) and the average salinity (*S*) of the Isohaline Layer (IHL) and the halocline in the Gerlache Strait. Data from WOA18 for the period 1981-2010.

Gerlache stations	Layer	Summer (DJF)		Autumn (MAM)		Winter (JJA)		Spring (SON)	
		Thickness, m	Average S	Thickness, m	Average S	Thickness, m	Average S	Thickness, m	Average S
G1	IHL	5	33.42	5	33.64	33	33.97	28	34.05
	Halocline	203	33.99	220	34.07	183	34.27	163	34.28
G2	IHL	5	33.60	5	33.68	50	33.96	43	34.28
	Halocline	195	34.05	195	34.04	150	34.20	140	34.28
G4	IHL	5	33.75	5	33.80	58	33.99	60	34.21
	Halocline	195	34.13	245	34.14	192	34.28	137	34.37
G8	IHL	5	33.88	10	33.88	45	34.01	67	34.25
	Halocline	178	34.19	215	34.17	195	34.32	123	34.38
G12	IHL	8	34.00	10	33.95	48	34.07	58	34.28
	Halocline	150	34.22	190	34.19	143	34.36	128	34.39

Thermocline, Halocline and Pycnocline

The seasonal variation of the thicknesses of the thermocline and the average value of *T* in areas of the Gerlache Strait are shown in Table 3. The greatest thickness occurs during southern summer in the northeast zone with 120 m in G8 and 220 m in G12 where the average *T* is 0.35 °C and 0.33 °C respectively. The smallest thickness is located in the southwest zone G1 with 63 m and 0.44 °C. The lowest thickness of the thermocline is recorded during the austral winter, being greater in the northeast zone with 13 m and an average *T* equal to -0.82 °C (G8) and less thick with 8 m in the central east zone, also with an average *T* of -0.82. °C (G4).

Table 4 presents the values of the halocline thickness and the seasonal mean of *S* in the Gerlache Strait stations. In the austral autumn the thickness of the halocline is greater, highlighting the highest value in the eastern central zone (G4) with 245 m and 34.14 *S*, and the lowest in the northeast zone (G12) with 190 m and 34.19. In spring, the halocline registers the smallest thickness of the year, being the greatest 163 m with 34.28 S in the southwest zone (G1), and the least with 123 m and 34.38 in the northeast zone (G8). Regarding the ϱ profiles, their values oscillate between 1027 and 1030 kg/m³. As you go down in the water column ϱ increases from about 1027 kg/m³ at the surface to 1030 kg/m³ at 300 m. It is proposed that the pycnocline ranges from 5 to 300 m throughout the year.

Bottom Layer

In the austral summer the upper limit of the BL from the thermal point of view is deeper in the north than in the south of the Strait of Gerlache, the highest average *T* for the BL is found in the southwest zone and the lowest in the northeast area. In winter, the upper limit of the BL is at approximately the same depth both north and south of the Gerlache Strait, with the highest average *T* for the BL being in the southwest and the lowest in the northeast. Taking into account the *S*, in the austral summer the upper limit of the BL is found at a greater depth in the southwest zone (G1) compared to the northeast zone (G8 and G12), higher average *S* for BL is observed in the Southwest area compared to the Northeast area. In winter, the upper limit of the BL is deeper in the central east (G4) and northeast (G8) zones, the highest average *S* for this layer is observed in the northeast zone and the lowest in the southwest zone (Table 5).

Table 5. Depth (*Z*, m) of the upper limit of the Lower Layer (BL), Temperature (*T*, °C) and Salinity (*S*) in austral summer and winter in the Gerlache Strait. WOA18 data for the period 1981-2010.

Gerlache stations	Summer (DJF)				Winter (JJA)			
	BL by Temperature		BL by Salinity		BL by Temperature		BL by Salinity	
	Upper Lim., m	T, °C	Upper Lim., m	S	Upper Lim., m	T, °C	Upper Lim., m	S
G1	70	-0.12	208	34.56	10	-1.22	217	34.57
G2	83	-0.08	-	-	12	-1.24	-	-
G4	108	-0.14	200	34.51	8	-1.36	250	34.56
G8	125	-0.27	183	34.49	7	-1.32	242	34.63
G12	225	-0.33	158	34.45	10	-1.25	192	34.65

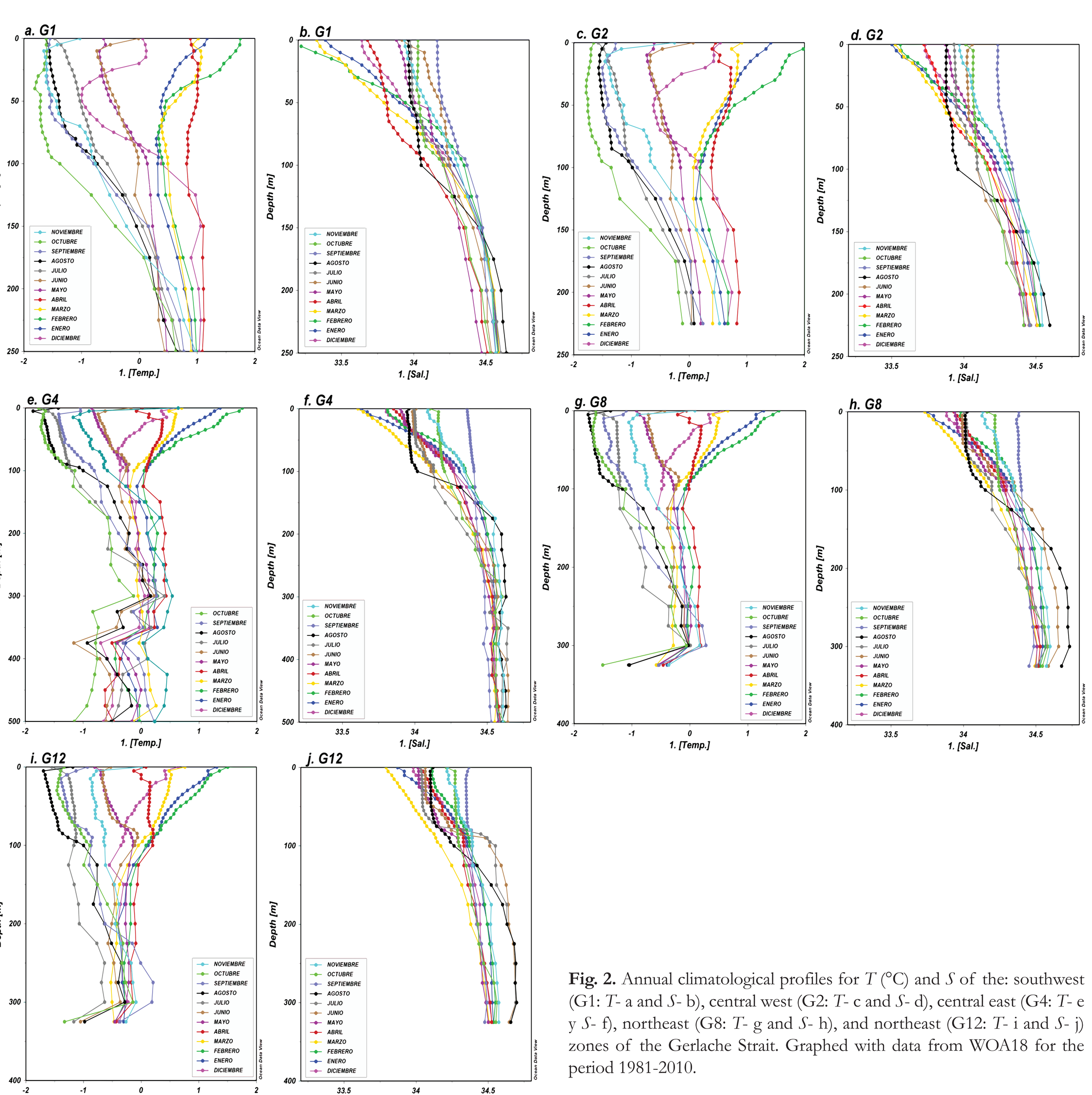

Fig. 2. Annual climatological profiles for *T* (°C) and *S* of the: southwest (G1: *T*- a and *S*- b), central west (G2: *T*- c and *S*- d), central east (G4: *T*- e y *S*- f), northeast (G8: *T*- g and *S*- h), and northeast (G12: *T*- i and *S*- j) zones of the Gerlache Strait. Graphed with data from WOA18 for the period 1981-2010.

Thermohaline stability for 1981-2010 along the Gerlache Strait: Hesselberg-Svedrup criterion and Vaisala-Brunt Frequency.

The multi-year average *Et* profiles for stations G1, G2, G4, G8 and G12 from the period 1981-2010 are shown in Fig. 3a. In the first 100 m, the contribution of *Et* begins to recede from positive values close to zero on the surface to a negative peak at 100 m, evidenced mainly in G2. Below 100 m, the contribution of *Et* to total *E* is constant and with negative values, oscillating around -2x10-7 kg/m⁴ and 0 kg/m⁴ between 100 and 200 m. Subsequently *Et* approaches zero at depths greater than 220 m. It is proposed that the stability condition for the water column according to the thermal input *Et* is: stable from 0 to 50 m and unstable for depths greater than 50 m. During the year *Et* is stable (Et>0) only in January and February and unstable (*Et*<0) in autumn, winter and spring.

The multi-year average *Es* profiles for the period 1981-2010 for stations G1, G2, G4, G8, and G12 are shown in Fig. 3b. In the first 100 m, the contribution of *Es* to stability begins with values greater than 0.05 kg/m⁴ and less than 0.15 kg/m⁴. As you descend, the *Es* values increase and presents an abrupt positive peak in the five profiles at 100 m. Below 100 m, the contribution of *Es* to total *E* decreases to values close to 0.05 kg/m4 around 200 m, then *Es* stabilizes with values very close to zero for depths greater than 300 m. Therefore, it is proposed that the *Es* condition for the water column according to the saline contribution is: stable from 0 to 300 m and indifferent to depths greater than 300 m. During the year, *Es* presents stability (*Es*>0) all along the year with the exception of spring, especially during September, when negative gradients of *S* and *Es*<0 are normally observed in the first 25 m of the water column.

Total Stability and Vaisala-Brunt Frequency

The multi-year average *E* profiles for stations G1, G2, G4, G8, and G12 for the period 1981-2010 are shown (Fig. 3c). It is observed that the *E* curves are largely identical to the curves of the salt component *Es*. When calculating the total stability *E* = *Et* + *Es*, the *Et* component can be considered negligible, since its values affect the total *E* very little. Thus, *E* ≈ *Es*.

As previously mentioned in the description, at 100 m depth a positive abrupt peak is observed for *Es* and *E* regardless of the season, and a negative peak for *Et* at the same depth. This notable positive *S* and negative *T* peak at 100 m appears to be related to the intrusion of a warmer, saltier water mass through the Bismarck Strait, as evidenced by longitudinal transects of *T*. It is proposed that the condition of *E* for the water column is: stable from 0 to 300 m and indifferent for depths greater than 300 m.

Considering the profiles for N of the multi-year average for stations G1, G2, G4, G8, and G12 of the base period 1981-2010 (Fig. 3d). The values of N begin to increase, oscillating between 0.008 s⁻¹ and 0.0095 s⁻¹ between 0 and 100 m for the five stations. As the depth of the water column is lowered regardless of the season, the five curves reach their maximum range of oscillation near 100 m depth. Between 100 m and 400 m depth the opposite is observed, the oscillation ranges begin to decrease considerably for all the curves, contracting from 0.008 s⁻¹ to 0.007 s⁻¹ as one descends in the vertical.

Values of *N* of the order of 0.001 s⁻¹ are observed and the curves stabilize at 0.007 s⁻¹ or close values for depths greater than 300 m for the selected stations. Therefore, it is proposed that these values of oscillation of the frequency *N* indicate that in the study region there are water mixing processes mainly at the surface level (0-100) m, to a greater extent in the summer seasons and in a lesser extent in winter. It is possible to identify that the oscillations of *N* are closely related to the fluctuations of the stability *E*.

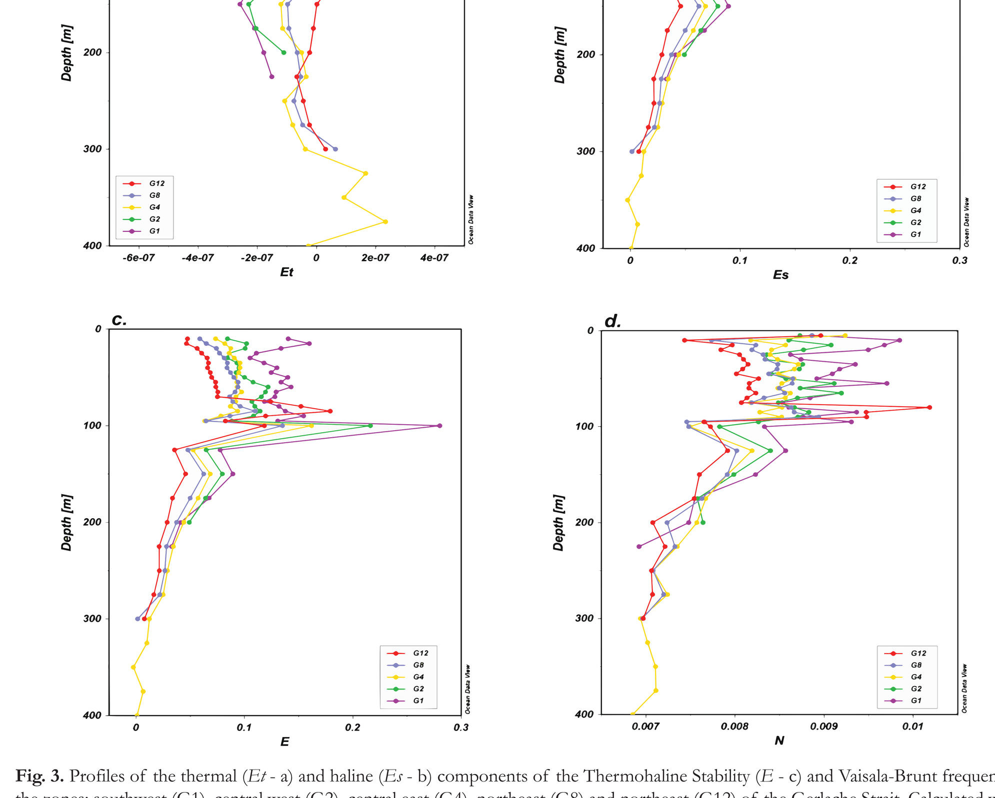

Fig. 3. Profiles of the thermal (*Et* - a) and haline (*Es* - b) components of the Thermohaline Stability (*E* - c) and Vaisala-Brunt frequency (*N* - d) for the zones: southwest (G1), central west (G2), central east (G4), northeast (G8) and northeast (G12) of the Gerlache Strait. Calculated with data from WOA18 for the period 1981-2010.

Fine structure

Based on the parameters and criteria for the determination of different predominant fine structure mechanisms exposed in the methodology, the fine structure along the Strait of Gerlache is shown for G1, G2, G4, G8 and G12 in the form of a longitudinal transect for the multi-year average for the period 1981-2010 (Table. 6). In the southwest zone G1, total or absolute stability (AS) predominates in the layers above 55 m, and below 55 m, stratification by type of convection per layer (CL) is observed. Likewise, in the centralwest zone G2, AS prevails above 65 m and CL is evident below 65 m. In the centraleast zone G4, AS predominates in layers above 70m, between 70 and 325 m CL occurs, followed by AS again between 325 and 375 m, and between 375-400 there is stratification by SF, finally, below 400 m, CL dominates. In the northeast G8 zone, AS predominates in the layers above 70 m, between 70 and 300 m CL prevails, followed by SF between 300 and 325 m. In the northeast G12 zone, AS predominates in the layers above 60 m, between 60 and 90 m CL is observed, followed by AS between 90 and 150 m, and below 150 m CL dominates again. Summarising, in the Gerlache Strait the layers above 60 m are characterized by presenting AS, below 60 m CL prevails, stratification by SF is observed only between 300 to 325 m and 375 to 400 m in the stations G4 and G8 respectively.

Table 6. Longitudinal transect G1-G2-G4-G8-G12 of the fine structure mechanisms in layers of the Gerlache Strait for 1981-2010 calculated with data from WOA18. AS- Total or absolute stability, CL- Stratification by convection by layers, SF- Stratification by saline fingers.

Layers, m	G1	G2	G4	G8	G12
0-5	AS	AS	AS	AS	AS
5-10	AS	AS	AS	AS	AS
10-15	AS	AS	AS	AS	AS
15-20	AS	AS	AS	AS	AS
20-25	AS	AS	AS	AS	AS
25-30	AS	AS	AS	AS	AS
30-35	AS	AS	AS	AS	AS
35-40	AS	AS	AS	AS	AS
40-45	AS	AS	AS	AS	AS
45-50	CC	AS	AS	AS	AS
50-55	AS	AS	AS	AS	AS
55-60	CC	AS	AS	AS	AS
60-65	CC	AS	AS	AS	CC
65-70	CL	CC	AS	AS	CC
70-75	CL	CL	CL	CL	CL
75-80	CL	CL	CL	CL	CL
80-85	CL	CL	CL	CL	CL
85-90	CL	CL	CL	CL	CL
90-95	CL	CL	CL	CL	AS
95-100	CL	CL	CL	CL	AS
100-125	CL	CL	CL	CL	AS
125-150	CL	CL	CL	CL	AS
150-175	CL	CL	CL	CL	CL
175-200	CL	CL	CL	CL	CL
200-225	CL	CL	CL	CL	CL
225-250	CL		CL	CL	CL
250-275			CL	CL	CL
275-300			CL	CL	CL
300-325			CL	SF	AS
325-350			AS		
350-375			AS		
375-400			SF		
400-425			CL		
425-450			CL		
450-475			CL		
475-500			AS		

DISCUSSION

According to Kerr et al. (2018), during the Nautilus I expedition in February 2015, warmer *SSTs* were observed between the Brabant and Anvers islands (Schollaert channel), that is, the central west zone (G2) and in the northern sector of Gerlache, except for the transition zone between the Gerlache and Bransfield Straits (G10-G12). The authors mention that there was a relatively small difference in the average *SST* between the northern and southern Gerlache sectors, mainly due to processes such as: intrusions of warmer water masses, melting of sea ice and melting of glaciers. According to Hernández et al. (2021), the *SST* presents a monomodal behavior to the WAP, with high values in February and a minimum in August. In the Gerlache Strait, the *SST* values decrease from the northeast (G8 and G12), towards the southeast (G1 and G2), observing in the region an accentuated difference between north and south values at the end of spring and summer.

Likewise, in Kerr et al. (2018) the distribution of the *SSS* shows a marked influence of high salinity waters transported from the Bransfield Strait in a northeasterly direction to the Gerlache Strait (G10-G12). An increase in the proportion of fresh water due to glacial melting in the southwest zone (G1) is mentioned, which results, on average, in slightly saltier surface waters in the northeast zone (G12), results that agree with those observed in the present study.

Regarding the layers that make up the water column, ITL and IHL have an average depth of 50 m, these layers are in constant contact with the atmosphere, solar radiation, wind action and currents, being exposed to active turbulence. that standardizes their physicochemical properties (Garrison 2009), they present seasonal cooling and heating cycles that can be evidenced in the *T* and *S* profiles (Fig. 2). During the autumn in the months of March and April (Table 3) the ITL has its greatest thickness. In the spring months, specifically September (Table 4), the IHL has its greatest thickness.

A thermocline with a maximum thickness is observed during the austral summer in February, with an approximate thickness of 95 m in the central zone (Figs. 2c and 2e), and a thermocline of minimum or non-existent thickness throughout the austral winter, when the water column presents thermal instability. The halocline has a maximum thickness in autumn, with an approximate thickness of 220 m in the central zone (Figs. 2d and 2f) in April and a minimum in spring with a thickness of approximately 105 m in the central zone in September. The pycnocline is constituted as a permanent layer throughout the year for the studied water column and has an approximate thickness of 300 m. The details of each of the layers are recorded in (Tables 3-5). In the BL the *T* are low, the *S* are high and the ϱ are high, the vertical gradients dT/dz and dS/dz are close to zero, and an almost rectilinear vertical profile of *T*, *S* and ϱ is distinguished due to the fact that the parameters stabilize around a constant value as one descends in the water column.

According to Garcia et al. (2002), the ranges of *T* between -1.8 to 1.0 °C and *S* between 33.0 to 33.7, correspond to the so-called Antarctic Surface Water (**AASW**), the waters in the Gerlache Strait above 100-150 m are made up mainly of **AASW**. The dispersion of values in the profiles of *T* and *S* (Fig. 2) in the first 150 m of the water column illustrate the temporal and spatial variation that occurs at **AASW** during the year. **AASW** shows a wide range of *T* and *S* because it is affected by a wide variety of mechanisms, including atmospheric exchange, sea ice formation and melting, and exchanges along the permanent pycnocline (Smith et al., 1999). These changes create considerable variability in **AASW** throughout the year.

During the austral winter a layer of cold and homogeneous water with *T* below -1.5 °C, between 0 and 50m, corresponds to the QHL in winter. In Garcia et al. (2002), it is stated that values of *T* less than -1.5 °C and *S* in the range of 33.8-34.0 are associated with Winter Water (**WW**), considered the terminal part of **AASW**. This water mass is formed by the cooling of the most superficial portion of the water column during the winter season. **WW** in the *T*-transects (not shown in this poster) ranges from 0 to 50 m, subsequently **WW** is eroded by mixing and seasonal heating of the water column during spring and summer.

According to Garcia et al. (2002) the data points that present T above 1.0°C and S between 34.60 and 34.73 at depths below 200 m represent Circumpolar Deep Water (CDW), CDW is divided into two types, Upper Circumpolar Deep Water (UCDW) and Lower Circumpolar Deep Water (LCDW), which reflect different properties and depths (Smith et al., 1999). In the Antarctic Peninsula **UCDW** surges to the continental shelf and mixes with **AASW** to form a modified version of UCDW called (**mUCDW**) (Venables et al., 2017). The values presented in Tables 3 and 4 could evidence the intrusion of **mUCDW** between 250 and 500 m southwest (G1) of the Gerlache Strait.

In a more recent study Torres et al. (2020) also indicate that the relatively warm, salty and poorly oxygenated modified Circumpolar Deep Water (**mCDW**) penetrates the continental shelf and dominates the Bismarck Strait, from where they proceed to enter the Gerlache Strait, especially through its southwest entrance (G1). Likewise, the openings between the islands of the Palmer Archipelago (G4) along the Gerlache Strait also provide connections with the shelf to the west of the Antarctic Peninsula through which **mUCDW** can enter (Torres et al., 2020).

Moreover, in longitudinal transects of *T*, it was possible to visualize the intrusion of the High Salinity Shelf Water (**HSSW**), in the northeast region (G12) of the Gerlache Strait, where a body of *T* water is observed below the - 0.5 °C between 300 and 500 m during summer and autumn. The **HSSW** forms in the Weddell Sea and moves south along the deep basins of Bransfield Strait, entering Gerlache Strait through its northern boundary. As denser and cooler **HSSW** flows through deep channels in the bathymetry connecting deep basins in the Bransfield and Gerlache Straits, its properties change to form modified High Salinity Shelf Waters (**mHSSW**) (Torres et al., 2020).

The *E* of the water column was evaluated using the Hesselberg-Svedrup criteria and the Vaisala-Brunt Frequency. In the vertical profiles of the total thermo-haline contribution *E* (Fig. 3c), it is observed that the curves of *E* are largely identical to the curves in *Es* (Fig. 3a). It is concluded that the contribution of *Et* (Fig. 3b) is considered negligible, since it includes very small values compared to the contributions of *Es*, that means *E* ≈ *Es*, it's proposed that the stability condition for the water column is: stable from 0 to 300 m and indifferent for depths greater than 300 m. Also, it is proposed that according to the oscillation values of *N* (Fig. 3d), water mixing processes should occur mainly at the surface level, to a greater extent in summer and to a lesser extent in winter. It is also possible to correlate the high oscillations of *N* and the peaks of the *E* curves at 100 m, with the intrusion of **mUCDW**.

To date there are no studies in the literature concerning the fine structure in the Gerlache Strait. With regard to this structure (Fig. 4) findings in the Gerlache Strait it shows a similar configuration in both longitudinal and transversal sections, the layers above 60 m are characterized by presenting AS, below the 60 m CL prevails, and SF are observed only between 300 to 325 m and 375 to 400 m at some stations. A detailed characterization of the properties, distribution and annual climatological behavior of the water masses in the Gerlache Strait using reanalysis data is proposed for future research.

CONCLUSIONES

The month of February registers the highest *SST*, reaching 2.0 °C in the centralwest zone (G2). During the month of October, the lowest *SST* is recorded with -1.84°C at the entrance to the southwestern zone, ending with the Bismarck Strait and beginning with the Gerlache Strait (G1). The highest *SSTs* are recorded in the centralwest region of the strait (G2) and the lowest in the northeast region (G9).

The month of September registers the highest *SSS* with 34.4 in the centraleast region (G5). The lowest *SSS* is recorded in the month of February with 33.19 in the southwest region (G1). During the course of the year, the highest *SSS* is recorded in the northeast area of the strait (G12) and the lowest in the southwest (G1).

A thermocline with a maximum thickness is observed for the summer months, with an approximate thickness of 90 m in the central zone and a thermocline of minimal thickness or non-existent for the winter months, in which the water column presents thermal instability. The halocline has a maximum thickness for autumn, with a thickness of 220 m in the central area and a minimum for the spring, with 105 m in the central area. The pycnocline is constituted as a permanent layer throughout the year for the studied water column and has a thickness equal to or greater than 300 m.

The first 150 m *T* and *S* profiles of the water column illustrate the temporal and spatial variation that occurs at **AASW** during the course of the twelve months of the year. In longitudinal transects of *T* and *S*, the intrusion of **mUCDW** is evident between 250 and 500 m southwest (G1) of the Gerlache Strait. In longitudinal transects of *T*, the intrusion of **mHSSW** is evident between 300 and 500 m northeast (G12) of the Gerlache Strait.

Considering that *E* ≈ *Es*, it is proposed that the total thermohaline stability condition of the water column is: stable from 0 to 300 m and indifferent for depths greater than 300 m. The *N* oscillation values indicate water mixing processes mainly at the surface level, to a greater extent in summer and to a lesser extent in winter. Finally, regarding the fine structure, the layers above 60 m are characterized by presenting AS, below 60 m stratification by CL prevails, and stratification by SF is observed only between 300 and 325 m, 325 to 350 m and 375 to 400 m in some stations.

REFERENCES

García, M. A., Castro, C. G., Ríos, A. F., Doval, M. D., Rosón, G., Gomis, D., & López, O. (2002). Water masses and distribution of physico-chemical properties in the Western Bransfield Strait and Gerlache Strait during Austral summer 1995/96. Deep-Sea Research Part II: Topical Studies in Oceanography, 49(4–5), 585–602. https://doi.org/10.1016/S0967-0645(01)00113-8.

Garrison, T. (2009). Essentials of Oceanography, Fifth Edition. In Brooks/Cole, Cengage Learning.

Hernández, M., Villegas, N., & Concha, A. (2021). Descripción general de algunas variables meteo-marinas de aguas superficiales adyacentes al archipiélago de Palmer, península Antártica, durante 1979-2018 con base en datos Era5. Boletín de Investigaciones Marinas y Costeras, 50(1), 141–162.

Kerr, R., Orselli, I. B. M., Lencina-Avila, J. M., Eidt, R. T., Mendes, C. R. B., da Cunha, L. C., Goyet, C., Mata, M. M., & Tavano, V. M. (2018). Carbonate system properties in the Gerlache Strait, Northern Antarctic Peninsula (February 2015): I. Sea–Air CO2 fluxes. Deep-Sea Research Part II: Topical Studies in Oceanography, 149(xx), 171–181. https://doi.org/10.1016/j.dsr2.2017.02.008.

Locarnini, R. A., Mishonov, A. V., Baranova, O. K., Boyer, T. P., Zweng, M. M., Garcia, H. E., Reagan, J. R., Seidov, D., Weathers, K. W., Paver, C. R., & Smolyar, I. V. (2019). World Ocean Atlas 2018. Volume 1: Temperature. NOAA National Centers for Environmental Information, 1, 1–43.

Smith, D. A., Hofmann, E. E., Klinck, J. M., & Lascara, C. M. (1999). Hydrography and circulation of the West Antarctic Peninsula Continental Shelf. Deep-Sea Research Part I: Oceanographic Research Papers, 46(6), 925–949. https://doi.org/10.1016/S0967-0637(98)00103-4.

Torres Parra, R. R., Caicedo Laurido, A. L., & Iriarte Sánchez, J. D. (2020). Hydrographic conditions during two austral summer situations (2015 and 2017) in the Gerlache and Bismarck straits, northern Antarctic Peninsula. Deep-Sea Research Part I: Oceanographic Research Papers, 161. https://doi.org/10.1016/j.dsr.2020.103278.

Venables, H. J., Meredith, M. P., & Brearley, J. A. (2017). Modification of deep waters in Marguerite Bay, western Antarctic Peninsula, caused by topographic overflows. Deep-Sea Research Part II: Topical Studies in Oceanography, 139, 9–17. https://doi.org/10.1016/j.dsr2.2016.09.005.

Zhou, M., Niiler, P. P., & Hu, J. H. (2002). Surface currents in the Bransfield and Gerlache Straits, Antarctica. Deep-Sea Research Part I: Oceanographic Research Papers, 49(2), 267–280. https://doi.org/10.1016/S0967-0637(01)00062-0.

Zweng, M. M., J. R. Reagan, D. Seidov, T. P. Boyer, R. A. Locarnini, H. E. Garcia, A. V. Mishonov, O. K. Baranova, K. Weathers, C. R. Paver, and I. Smolyar, 2018. World Ocean Atlas 2018, Volume 2: Salinity. A. Mishonov Technical Ed.; NOAA Atlas NESDIS 82, 50pp.